

Multiplexed phospholipid membrane platform for curvature sensitive protein screening

Eider Berganza, Mirsana P. Ebrahimkutty, Srivatsan K. Vasantham, Chunting Zhong, Alexander Wunsch, Alexander Navarrete, Milos Galic, Michael Hirtz

ELECTRONIC SUPPLEMENTARY INFORMATION

1. Gold nanoparticle on amine coated glass substrate

As a first approach to the realization of a lipid coated nanoparticle platform, a widely adopted method of NP anchoring on the substrate was trialed. Gold NPs were immobilized on an amine functionalized Surface (Fig. S1a), see experimental section for details). However, the approach was not stable enough for use in L-DPN, where the NPs are subjected to fairly high lateral forces during the patterning process. After covering the aminated glass surface with gold nanoparticles (Fig. S1b), AFM was performed as quality control. As it can be seen, the gold nanoparticle coating appears stable for applications that do not rely on applying high lateral forces on them.

After application of L-DPN, the sample was imaged again. Fig. S1c and d show topographic and phase AFM images of an intended square feature with a nanoparticle and lipid mixture dragged to the sides (marked with a blue arrow, also in the topographic profile shown in Fig S1e). The dragged out material accumulated especially on the right side, as a result of the left to right scanning of the DPN probe during lipid writing.

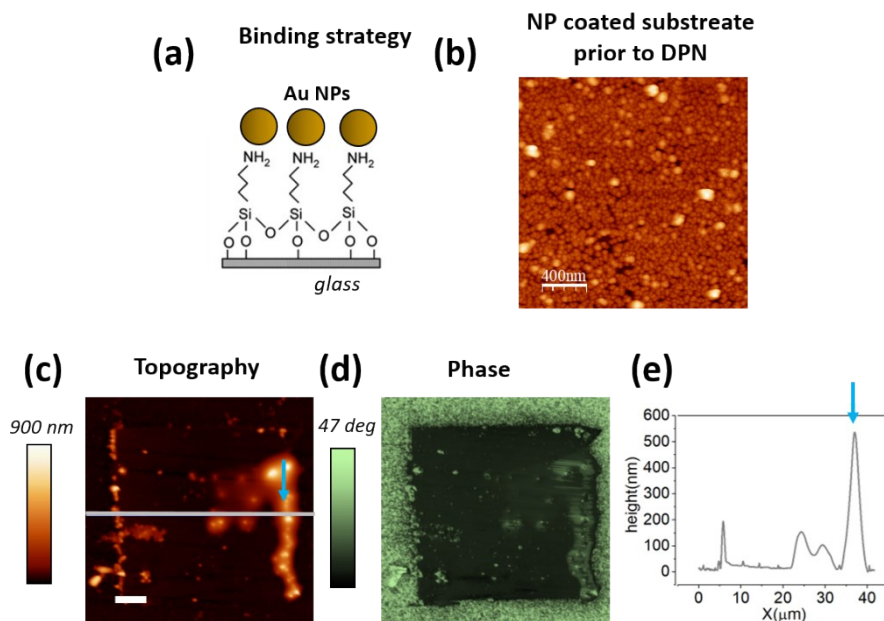


Fig. S1. a) Schematic representation of the chosen nanoparticles and substrate binding strategy. b) AFM image showing the state of the gold coated surface prior to DPN lithography. c) Topographic and d) phase image of gold nanoparticles detached from gold substrate during DPN patterning. e) The profile from the topographic image shows that the NPs and lipid material accumulate at the edges of the intended square.

2. The importance of cleaning gold substrates for silica nanoparticle anchoring

Cleaning the gold substrate before starting the coating process is a crucial step. For the experiments shown in this part samples have been used that were stored for up to a week after the gold was sputtered onto the glass substrate. Then, the substrates were subjected to different cleaning steps, prior to incubation with aminated silica nanoparticles (Fig.S2a). As one can see in Figure S2b, no anchoring of NPs is achieved, unless the surface is previously cleaned. Notice that in the AFM image a small roughness can be appreciated, which corresponds to sputtered gold grains of approximately 3 nm. Cleaning can be done either by wet chemical methods (e.g. piranha solution) or dry processes (e.g. O₂ plasma etching). In the given example (Fig. S2c), the gold coated substrate was immersed in piranha solution (H₂SO₄:H₂O₂) 70:30 vol % for 30 minutes. The surface coverage was quantified from the AFM images and it is calculated to be 44.8%. To ensure a coverage close to 100%, additional use of O₂ plasma was necessary (Fig. S2d). In general terms, samples close to full coverage were used for the experiments shown along the manuscript. Due to the well-known shortcomings

of AFM, regarding the tip geometry influence, we state that the surface coverage values might be overestimated.¹

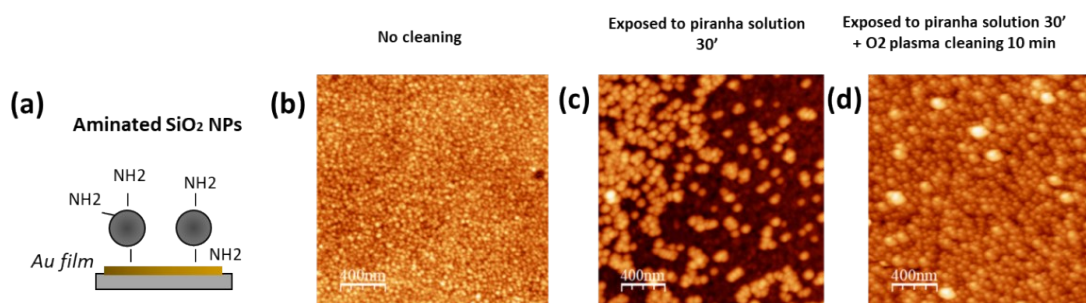


Figure S2. representation of the silica nanoparticles on gold substrate. b) AFM image showing no attachment of silica nanoparticles after incubation, when the gold surface is not cleaned. c) Gold surface with partial coverage of silica nanoparticles after the gold was cleaned with piranha solution prior to the nanoparticle coating. d) Gold surface fully covered with silica nanoparticles due to prolonged cleaning process prior to nanoparticle deposition.

3. Roughness

The roughness analysis can provide a deeper insight into the way the phospholipid molecules arrange on the nanoparticles. The root mean square deviation (RMS) is a widespread used parameter used to quantify surface roughness values in AFM measurement analysis.² It is calculated by the WSxM image analysis software³ using the following expression:

$$RMS = \sqrt{\sum_i \frac{(Z_i - Z_{avg})^2}{N}}$$

A sample with 1.5 bilayers of patterned phospholipids was selected to conduct a roughness analysis. Two areas, one with non-covered nanoparticles (Fig. S3a-c) and one with the phospholipid layers (Fig. S3d-f) were compared, obtaining 4.17 nm and 3.44 nm RMS values respectively. As one could intuitively argue, a smaller RMS value confirms that despite the flexible nature of the lipid bilayer, the patterned molecules do not entirely follow the

¹ Y. Chen, W. Huang, *Meas. Sci. Technol.* **2004**, *15*, 2005.

² S. J. Fang, W. Chen, T. Yamanaka, C. R. Helms, *Appl. Phys. Lett.* **1996**, *68*, 2837.

³ I. Horcas, R. Fernández, J. M. Gómez-Rodríguez, J. Colchero, J. Gómez-Herrero, A. M. Baro, *Rev. Sci. Instrum.* **2007**, *78*, 013705.

nanoparticle shape. As we mentioned in the previous section, the tip geometry also influences the calculated RMS values, as the final tip radius is close to the feature size.

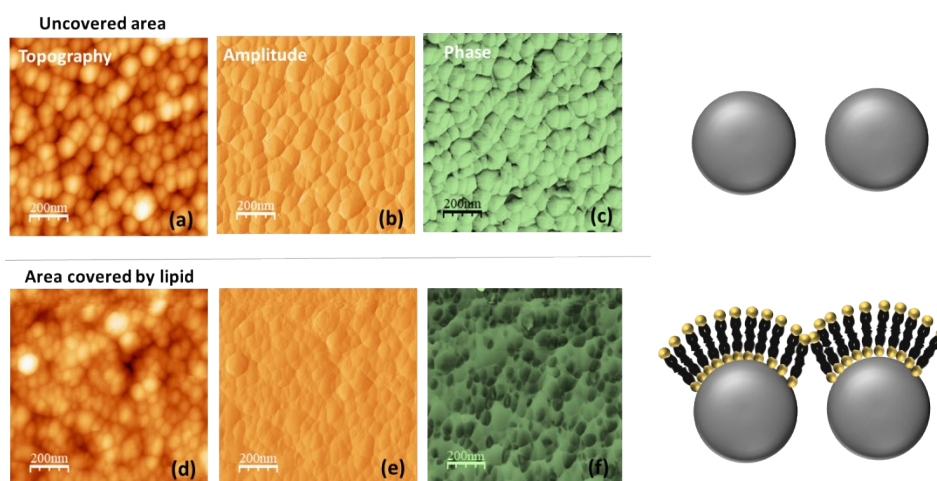


Figure S3. a), c) Topography b), d) amplitude and c), e) phase image of nanoparticle coated substrate area with and without phospholipid layer subsequently.

4. Adjusting writing parameters to obtain better nanoparticle coverage

Tuning of lipid patch thicknesses in L-DPN by adjusting the relative humidity and writing speed as process parameters is well established.^{4,5,6,7,8} Although in general, high nanoparticle density is desirable for protein sensing applications, a good nanoparticle coverage with lipids, regardless of the nanoparticle density can be achieved by creating thicker lipid patches (by raising the humidity or lowering the writing speed), with thicknesses beyond the nanoparticle radius. This is shown in Fig. S4, where Fig. S4a and S4c show a fully covered substrate with small density on nanoparticles, with lipid patches of different thicknesses patterned onto them. The phase image shows that no nanoparticle puncturing can be observed. In Fig. S4b, a 80 nm thick lipid patch is patterned onto a substrate fully covered with a higher nanoparticle density.

4 S. Lenhert, P. Sun, Y. Wang, H. Fuchs, and C.A. Mirkin, *Small* **2007** 3, 71.

5 S. Biswas, M. Hirtz, and H. Fuchs, *Small* **2011**, 7, 2081.

6 M. Hirtz, A. Oikonomou, T. Georgiou, H. Fuchs, and A. Vijayaraghavan, *Nat. Commun.* **2013**, 4, 2591.

7 A. Urtizberea, M. Hirtz, and H. Fuchs, *Nanofabrication* **2016**, 2, 43.

8 A. Urtizberea and M. Hirtz, *Nanoscale* **2015**, 7, 15618.

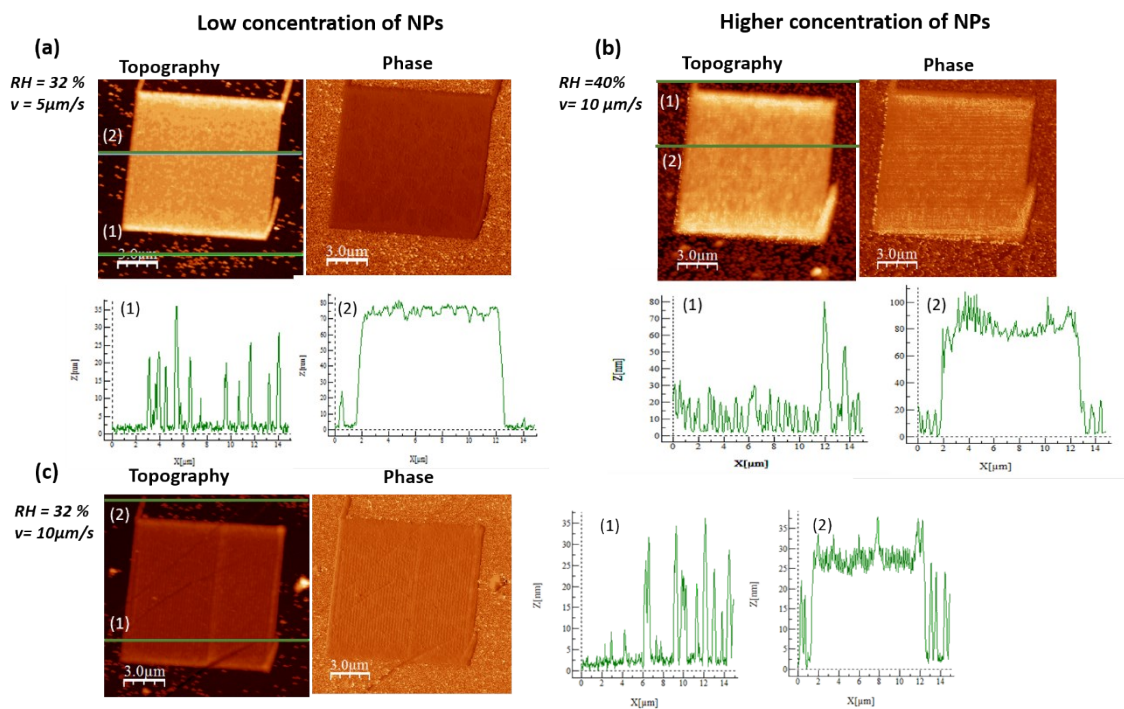


Figure S4. Lipid patches of different thicknesses patterned under different writing conditions for relative humidity and writing speed (conditions indicated on the left of each image set) onto substrates fully coated with 25nm nanoparticles. a) and c) present lower nanoparticle coverage and (b) presents higher nanoparticle coverage. None of the examples shows nanoparticle puncturing as is evidenced by comparing the profile lines given for each panel as (1) off the lipid patches showing the NP density and (2) on the lipid patch.

5. Water immersion

In a second experiment, we used fluorescently labelled bovine serum albumin (BSA), a protein frequently used for “blocking” sites of unspecific adhesion on substrates before functional proteins are incubated, to probe a freshly produced sample. As we can infer from Figure S5, the fluorescently labelled BSA is only visible around the lipid patches in the green channel, after the patches are incubated with BSA for 20 minutes. This is further evidence, that the lipid layers remain intact and in place under immersion, as they (exhibiting anti-fouling properties themselves) attract much less BSA as the bare NP substrate in the surrounding area.

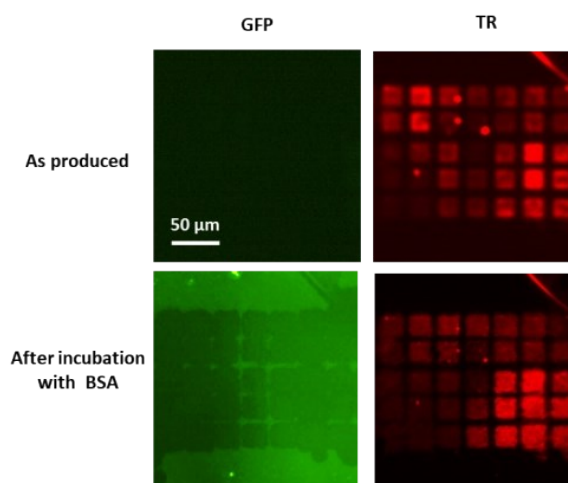


Figure S5. A sample covered with a lipid membrane array was imaged before and after BSA incubation. The green/GFP channel shows the BSA signal, the red/TR channel shows the rhodamine signal of the Rho-PE admixed to the patterned lipid.

6. Multiplexing and 25 nm nanoparticle spotting

To showcase the multiplexing capacity of the micro-contact spotting technique, two inks containing nanoparticles of different sizes were sequentially spotted: First, 100 nm nanoparticle dispersion was spotted (Fig. S6a), followed by a change of tip to complete the spotting of 25 nm nanoparticle dispersion in between the previously patterned spots.

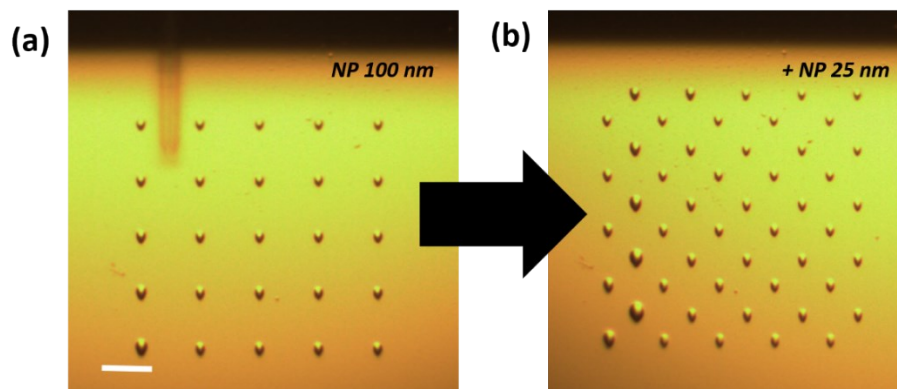


Figure S6. Optical microscopy image of a) 100 nm nanoparticle ink spotted on a gold surface and b) 25 nm nanoparticle ink spotted in between previously made spots. Scale bar is 50 μm .

The experiments to pattern 25 nm nanoparticles were performed with the same parameters used to spot 100 nm NPs, following the procedure described in the experimental section. The nanoscale image of the spots are shown in Figure S7.

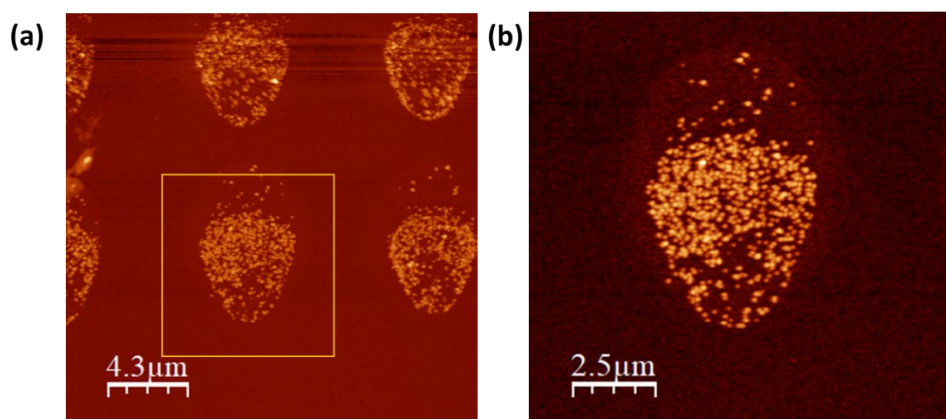


Figure S7. a) AFM image of a 25 nm spotted microarrays. b) Zoom the spotted area highlighted in a yellow square.

7. Curvature-dependent protein screening

On the first approach of the Nadrin-2 BAR domain binding experiments, negatively charged lipids were patterned on 100 nm diameter nanoparticle coated substrates. Notice that all lipid patches were initially fluorescently labelled (red) by an admixing of Rho-PE to the lipid ink, to make their localization easier during protein binding experiments. In addition, the Nadrin 2 is also fluorescently tagged with YFP (yellow fluorescent protein) for detection at 514 nm (green). In Figure S8, representative images as well as line scans through individual patches are shown. Labelled by arrows, local enrichment of YFP-positive protein puncta (green) within rhodamine-labelled membrane patches (red) are shown. As the Rho-PE is very bright compared to the protein, we observed some bleed-through in the green channel. To avoid this problem, the follow-up experiments and repetitions were implemented with non-fluorescently labelled phospholipids to bypass any crosstalk related artifacts. These results are reported in the main text.

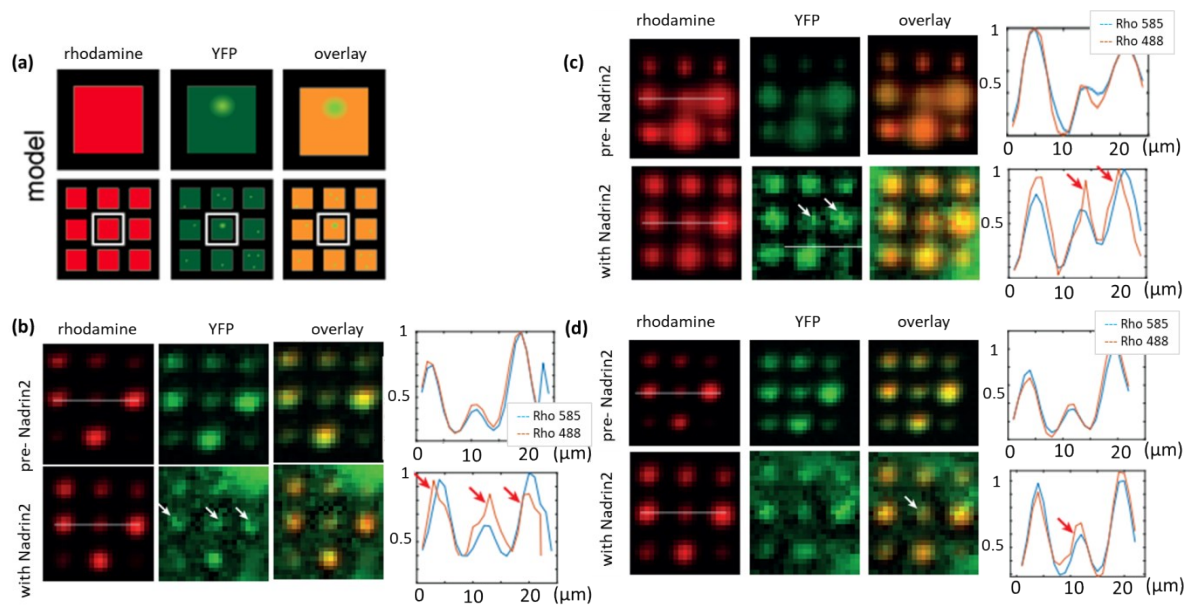


Figure S8. Nadrin 2 on Nanoparticles deposited with 70% DOPC and 30% POPS. a) Followed model. Obtained experimental results are shown in b), c) and d). Normalized intensity profiles are plotted against distance.

8- Negative control on flat substrates

A lipid mixture comprising 70:30 mol% DOPC:POPS with no fluorescent content were deposited on a flat gold surface and incubated with the Nadrin2 BAR domain (Fig. S9a). The results were then compared to those obtained on samples patterned on NP coated substrates (Fig. S9b). To probe for protein binding, the fluorescence intensity distribution of the images was compared. The negative control (Fig. S9a) showed no increase in fluorescence intensity at patches. Consistently, grey values of the image displayed gaussian distribution. In contrast, proteins enriched on locally curved substrates, as shown by the local increase in fluorescence intensity (Fig. S9b, top) and relative increase in pixels with high grey values (Fig. S9b, bottom).

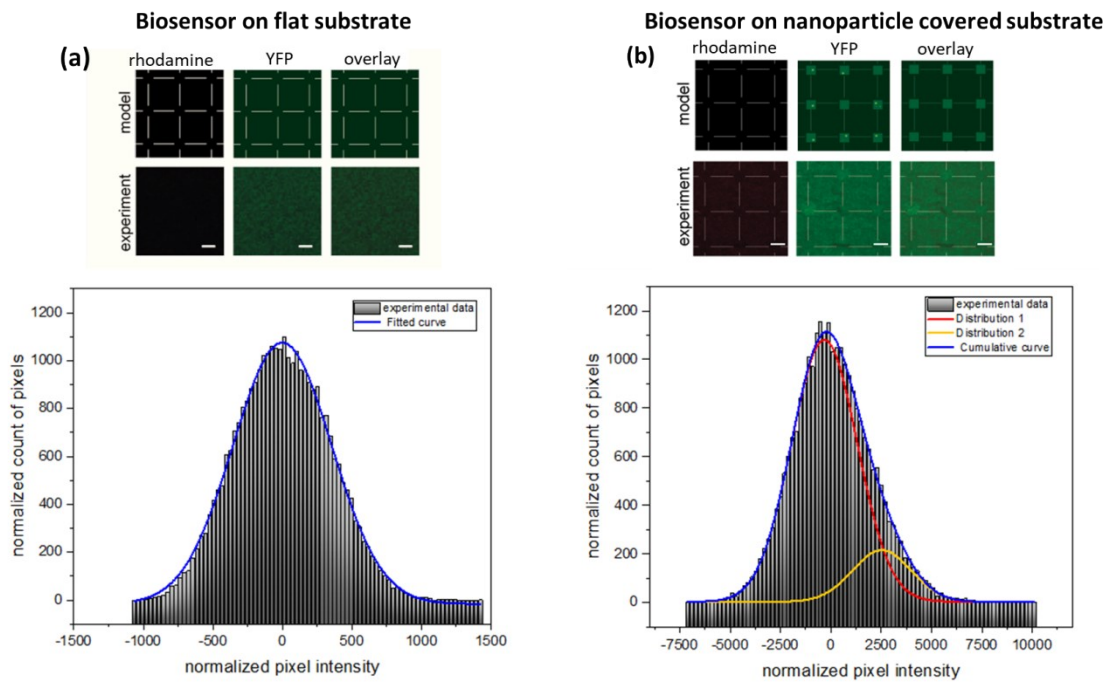


Figure S9. Measured fluorescent signals and corresponding histogram of the intensities of the YFP channels on a) flat and b) curved substrates. Scale bar 3 μm .